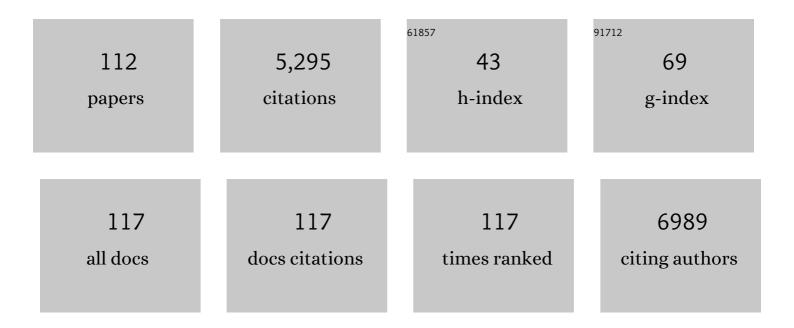
List of Publications by Year in descending order

Source: https://exaly.com/author-pdf/7610399/publications.pdf Version: 2024-02-01



LUNCHENC HU

#	Article	IF	CITATIONS
1	One-Pot Synthesis of CdS and Ni-Doped CdS Hollow Spheres with Enhanced Photocatalytic Activity and Durability. ACS Applied Materials & amp; Interfaces, 2012, 4, 1813-1821.	4.0	263
2	Sunflower and rapeseed oil transesterification to biodiesel over different nanocrystalline MgO catalysts. Green Chemistry, 2008, 10, 373-381.	4.6	238
3	In-situ topotactic synthesis and photocatalytic activity of plate-like BiOCl/2D networks Bi2S3 heterostructures. Applied Catalysis B: Environmental, 2018, 220, 570-580.	10.8	185
4	Synthesis and photocatalytic activity of BiOBr nanosheets with tunable exposed {0 1 0} facets. Applied Catalysis B: Environmental, 2016, 188, 283-291.	10.8	164
5	Efficient Preparation and Catalytic Activity of MgO(111) Nanosheets. Angewandte Chemie - International Edition, 2006, 45, 7277-7281.	7.2	149
6	Adsorption Properties of MgO(111) Nanoplates for the Dye Pollutants from Wastewater. Journal of Chemical & Engineering Data, 2010, 55, 3742-3748.	1.0	147
7	MgO(111) Nanosheets with Unusual Surface Activity. Journal of Physical Chemistry C, 2007, 111, 12038-12044.	1.5	133
8	NiO(111) nanosheets as efficient and recyclable adsorbents for dye pollutant removal from wastewater. Nanotechnology, 2009, 20, 275707.	1.3	119
9	Intercalation of Aggregation-Free and Well-Dispersed Gold Nanoparticles into the Walls of Mesoporous Silica as a Robust "Green―Catalyst for <i>n</i> -Alkane Oxidation. Journal of the American Chemical Society, 2009, 131, 914-915.	6.6	119
10	Er3+ doped bismuth molybdate nanosheets with exposed {010} facets and enhanced photocatalytic performance. Applied Catalysis B: Environmental, 2011, 110, 221-230.	10.8	119
11	Construction of CdS/CoOx core-shell nanorods for efficient photocatalytic H2 evolution. Applied Catalysis B: Environmental, 2018, 234, 109-116.	10.8	117
12	Size-tunable fabrication of multifunctional Bi2O3 porous nanospheres for photocatalysis, bacteria inactivation and template-synthesis. Nanoscale, 2014, 6, 5402.	2.8	115
13	Ultrathin SnS2 nanosheets with exposed {001} facets and enhanced photocatalytic properties. Acta Materialia, 2014, 66, 163-171.	3.8	104
14	TiO <sub>2</sub> Nanoflakes Modified with Gold Nanoparticles as Photocatalysts with High Activity and Durability under near UV Irradiation. Journal of Physical Chemistry C, 2010, 114, 1641-1645.	1.5	98
15	Preparation and Surface Activity of Singleâ€Crystalline NiO(111) Nanosheets with Hexagonal Holes: A Semiconductor Nanospanner. Advanced Materials, 2008, 20, 267-271.	11.1	90
16	Aerobic oxidation of cyclohexane by gold nanoparticles immobilized upon mesoporous silica. Catalysis Letters, 2005, 100, 195-199.	1.4	87
17	Triplex Au–Ag–C Core–Shell Nanoparticles as a Novel Raman Label. Advanced Functional Materials, 2010, 20, 969-975.	7.8	87
18	Aerobic oxidation of alcohols catalyzed by gold nano-particles confined in the walls of mesoporous silica. Catalysis Today, 2007, 122, 277-283.	2.2	86

#	Article	IF	CITATIONS
19	Synthesis and characterization of tungsten-substituted SBA-15: An enhanced catalyst for 1-butene metathesis. Microporous and Mesoporous Materials, 2006, 93, 158-163.	2.2	82
20	General strategy for one-pot synthesis of metal sulfide hollow spheres with enhanced photocatalytic activity. Applied Catalysis B: Environmental, 2012, 125, 180-188.	10.8	80
21	Construction of NH2-MIL-125(Ti)/CdS Z-scheme heterojunction for efficient photocatalytic H2 evolution. Journal of Hazardous Materials, 2021, 405, 124128.	6.5	78
22	β-Bi2O3 and Er3+ doped β-Bi2O3 single crystalline nanosheets with exposed reactive {001} facets and enhanced photocatalytic performance. Applied Catalysis B: Environmental, 2013, 140-141, 141-150.	10.8	77
23	Cysteine modified anatase TiO2 hollow microspheres with enhanced visible-light-driven photocatalytic activity. Journal of Molecular Catalysis A, 2012, 356, 78-84.	4.8	74
24	Bubble template synthesis of copper sulfide hollow spheres and their applications in lithium ion battery. Materials Letters, 2012, 68, 28-31.	1.3	73
25	Plasma-assisted catalysis total oxidation of trichloroethylene over gold nano-particles embedded in SBA-15 catalysts. Applied Catalysis B: Environmental, 2007, 76, 275-281.	10.8	70
26	Bi metal-modified Bi <sub>4</sub> O <sub>5</sub> I <sub>2</sub> hierarchical microspheres with oxygen vacancies for improved photocatalytic performance and mechanism insights. Catalysis Science and Technology, 2017, 7, 3580-3590.	2.1	68
27	Controlled strategy to synthesize SnO2 decorated SnS2 nanosheets with enhanced visible light photocatalytic activity. CrystEngComm, 2012, 14, 5627.	1.3	65
28	Synthesis and characterization of Ni doped SnO <sub>2</sub> microspheres with enhanced visible-light photocatalytic activity. RSC Advances, 2015, 5, 56401-56409.	1.7	64
29	Facile solvent-thermal synthesis of ultrathin MoSe2 nanosheets for hydrogen evolution and organic dyes adsorption. Applied Surface Science, 2017, 402, 277-285.	3.1	62
30	Surfactant-mediated synthesis of single-crystalline Bi <sub>3</sub> O <sub>4</sub> Br nanorings with enhanced photocatalytic activity. Journal of Materials Chemistry A, 2017, 5, 15706-15713.	5.2	59
31	Controllable synthesis of highly active BiOCl hierarchical microsphere self-assembled by nanosheets with tunable thickness. Applied Catalysis B: Environmental, 2015, 172-173, 91-99.	10.8	57
32	Mass Production and Photocatalytic Activity of Highly Crystalline Metastable Single-Phase Bi <sub>20</sub> TiO <sub>32</sub> Nanosheets. Environmental Science & Technology, 2010, 44, 8698-8703.	4.6	55
33	Generalized Synthesis of Ternary Sulfide Hollow Structures with Enhanced Photocatalytic Performance for Degradation and Hydrogen Evolution. ACS Applied Materials & Interfaces, 2018, 10, 17911-17922.	4.0	55
34	Effect of La2O3-dopping on the Al2O3 supported cobalt catalyst for Fischer-Tropsch synthesis. Journal of Molecular Catalysis A, 2010, 330, 10-17.	4.8	54
35	Construction of Hierarchical MoSe <sub>2</sub> Hollow Structures and Its Effect on Electrochemical Energy Storage and Conversion. ACS Applied Materials & Interfaces, 2018, 10, 25483-25492.	4.0	53
36	Synthesis and surface activity of single-crystalline Co3O4 (111) holey nanosheets. Nanoscale, 2010, 2, 1657.	2.8	51

#	Article	IF	CITATIONS
37	Gold Nanoparticles Intercalated into the Walls of Mesoporous Silica as a Versatile Redox Catalyst. Industrial & Engineering Chemistry Research, 2011, 50, 13642-13649.	1.8	49
38	Nitrogen-doped graphene/CdS hollow spheres nanocomposite with enhanced photocatalytic performance. Chinese Journal of Catalysis, 2013, 34, 2138-2145.	6.9	48
39	Synthesis and visible light responsed photocatalytic activity of Sn doped Bi <sub>2</sub> S <sub>3</sub> microspheres assembled by nanosheets. RSC Advances, 2016, 6, 39810-39817.	1.7	46
40	Application and Properties of Microporous Carbons Activated by ZnCl <sub>2</sub> : Adsorption Behavior and Activation Mechanism. ACS Omega, 2020, 5, 9398-9407.	1.6	46
41	Title is missing!. Catalysis Letters, 2002, 81, 107-112.	1.4	45
42	Gram-scale wet chemical synthesis of wurtzite-8H nanoporous ZnS spheres with high photocatalytic activity. Applied Catalysis B: Environmental, 2011, 106, 212-219.	10.8	45
43	Synthesis and characterization of single-crystalline Bi <sub>2</sub> O <sub>2</sub> SiO <sub>3</sub> nanosheets with exposed {001} facets. Catalysis Science and Technology, 2017, 7, 3791-3801.	2.1	44
44	Synthesis and characterization of visible light responsive Bi3NbO7 porous nanosheets photocatalyst. Applied Catalysis B: Environmental, 2016, 196, 127-134.	10.8	43
45	Experimental and DFT studies of gold nanoparticles supported on MgO(111) nano-sheets and their catalytic activity. Physical Chemistry Chemical Physics, 2011, 13, 2582.	1.3	41
46	Mesoporous bimetallic PdCl2-CuCl2 catalysts for dimethyl carbonate synthesis by vapor phase oxidative carbonylation of methanol. Applied Catalysis A: General, 2003, 241, 363-373.	2.2	40
47	Novel Bi2O3/NaBi(MoO4)2 heterojunction with enhanced photocatalytic activity under visible light irradiation. Journal of Alloys and Compounds, 2013, 580, 475-480.	2.8	40
48	Synthesis and photocatalytic activity of porous bismuth oxychloride hexagonal prisms. Chemical Communications, 2016, 52, 994-997.	2.2	40
49	Catalytic Properties of Nanoscale Ironâ€Đoped Zirconia Solidâ€Solution Aerogels. ChemPhysChem, 2008, 9, 1069-1078.	1.0	39
50	Heterogeneous Wheelâ€Shaped Cu <sub>20</sub> â€Polyoxotungstate [Cu <sub>20</sub> Cl(OH) <sub>24</sub> (H <sub>2</sub> O) <sub>12</sub> (P <sub>8</sub> W <sub>48</sub> Catalyst for Solventâ€Free Aerobic Oxidation of <i>n</i> â€Hexadecane. Chemistry - A European Journal, 2009, 15, 7490-7497.	•O <sub>1 1.7</sub>	84 <i>s/s</i> ub>)] <s< td=""></s<>
51	A novel homogeneous catalyst made of poly(N-vinyl-2-pyrrolidone)-CuCl2 complex for the oxidative carbonylation of methanol to dimethyl carbonate. Journal of Molecular Catalysis A, 2002, 185, 1-9.	4.8	34
52	Self-assembly of layered wurtzite ZnS nanorods/nanowires as highly efficient photocatalysts. Journal of Materials Chemistry, 2011, 21, 16621.	6.7	34
53	Template-free synthesis of hollow core–shell MoO2 microspheres with high lithium-ion storage capacity. Materials Letters, 2012, 68, 82-85.	1.3	33
54	Controllable synthesis and morphology-dependent photocatalytic performance of anatase TiO <sub>2</sub> nanoplates. RSC Advances, 2015, 5, 513-520.	1.7	31

#	Article	IF	CITATIONS
55	Three-Dimensional Morphology Control during Wet Chemical Synthesis of Porous Chromium Oxide Spheres. ACS Applied Materials & Interfaces, 2009, 1, 1931-1937.	4.0	30
56	Co <sub>3</sub> O <sub>4</sub> Nanosheets with In-Plane Pores and Highly Active {112} Exposed Facets for High Performance Lithium Storage. Journal of Physical Chemistry C, 2017, 121, 19002-19009.	1.5	30
57	Synthesis of CdS hollow spheres coupled with g-C <sub>3</sub> N <sub>4</sub> as efficient visible-light-driven photocatalysts. Nanotechnology, 2016, 27, 355402.	1.3	29
58	Extraction of metal ions with non-fluorous bipyridine derivatives as chelating ligands in supercritical carbon dioxide. Journal of Supercritical Fluids, 2009, 51, 181-187.	1.6	26
59	Carbon Dioxide Reforming of Methane over Nickel Catalyst Supported on MgO(111) Nanosheets. Topics in Catalysis, 2014, 57, 619-626.	1.3	23
60	Construction of amorphous SiO2 modified β-Bi2O3 porous hierarchical microspheres for photocatalytic antibiotics degradation. Journal of Colloid and Interface Science, 2022, 607, 1717-1729.	5.0	23
61	Glutatione modified ultrathin SnS <sub>2</sub> nanosheets with highly photocatalytic activity for wastewater treatment. Materials Research Express, 2014, 1, 025018.	0.8	22
62	Hollow CdS nanotubes with ZIF-8 as co-catalyst for enhanced photocatalytic activity. Journal of Colloid and Interface Science, 2022, 606, 1882-1889.	5.0	22
63	Controllable Morphology and Photocatalytic Performance of Bismuth Silicate Nanobelts/Nanosheets. RSC Advances, 2011, 1, 1072.	1.7	21
64	Synthesis and photoactivity of the highly efficient Ag species/TiO2 nanoflakes photocatalysts. Journal of Alloys and Compounds, 2011, 509, 5152-5158.	2.8	21
65	Biomimetic structure design and construction of cactus-like MoS <sub>2</sub> /Bi <sub>19</sub> Cl <sub>3</sub> S <sub>27</sub> photocatalysts for efficient hydrogen evolution. Journal of Materials Chemistry A, 2018, 6, 21404-21409.	5.2	21
66	Strike a balance between adsorption and catalysis capabilities in Bi2Se3â^'xOx composites for high-efficiency antibiotics remediation. Chemical Engineering Journal, 2020, 382, 122877.	6.6	21
67	Enhancing potassium-ion battery performance by MoS2 coated nitrogen-doped hollow carbon matrix. Journal of Alloys and Compounds, 2021, 855, 157505.	2.8	21
68	Rational design of MoSe2 nanosheet-coated MOF-derived N-doped porous carbon polyhedron for potassium storage. Journal of Colloid and Interface Science, 2021, 600, 430-439.	5.0	21
69	Self-assembly of carbon nanotubes on a hollow carbon polyhedron to enhance the potassium storage cycling stability of metal organic framework-derived metallic selenide anodes. Journal of Colloid and Interface Science, 2021, 601, 60-69.	5.0	21
70	Synthesis and characterization of single-crystalline Bi <sub>19</sub> Cl <sub>3</sub> S <sub>27</sub> nanorods. Catalysis Science and Technology, 2017, 7, 3464-3468.	2.1	20
71	One-pot synthesis and electrochemical reactivity of carbon coated LiFePO4 spindles. Applied Surface Science, 2012, 263, 277-283.	3.1	19
72	Boosting potassium storage in nanosheet assembled MoSe2 hollow sphere through surface decoration of MoO2 nanoparticles. Applied Surface Science, 2020, 505, 144573.	3.1	19

#	Article	IF	CITATIONS
73	Hydrothermal synthesis of Mn-doped CdS hollow sphere nanocomposites as efficient visible-light driven photocatalysts. RSC Advances, 2015, 5, 15110-15117.	1.7	18
74	Engineering Amorphous Carbon onto Ultrathin g <sub>3</sub> N <sub>4</sub> to Suppress Intersystem Crossing for Efficient Photocatalytic H <sub>2</sub> Evolution. Advanced Materials Interfaces, 2018, 5, 1800859.	1.9	18
75	Surface Reconstruction-Associated Partially Amorphized Bismuth Oxychloride for Boosted Photocatalytic Water Oxidation. ACS Applied Materials & Interfaces, 2021, 13, 5088-5098.	4.0	18
76	Nanoscale gold intercalated into mesoporous silica as a highly active and robust catalyst. Nanotechnology, 2012, 23, 294010.	1.3	16
77	Carbon dots decorated on the ultrafine metal sulfide nanoparticles implanted hollow layered double hydroxides nanocages as new-type anodes for potassium-ion batteries. Chemical Engineering Journal, 2022, 433, 133539.	6.6	16
78	Controlled Synthesis of Nanoscale Icosahedral Gold Particles at Room Temperature. ChemCatChem, 2012, 4, 1662-1667.	1.8	15
79	Crucial Effect of Halogen on the Photocatalytic Hydrogen Evolution for Bi <sub>19</sub> X <sub>3</sub> S <sub>27</sub> (X = Cl, Br) Nanomaterials. Industrial & Engineering Chemistry Research, 2019, 58, 22958-22966.	1.8	15
80	Morphology-preserved transformation of CdS hollow structures toward photocatalytic H <sub>2</sub> evolution. CrystEngComm, 2020, 22, 1057-1062.	1.3	15
81	Highly efficient tungsten-substituted mesoporous SBA-15 catalysts for 1-butene metathesis. Materials Letters, 2006, 60, 3059-3062.	1.3	14
82	Zn <sub>0.8</sub> Cd <sub>0.2</sub> S Hollow Spheres with a Highly Dispersed Ni Dopant for Boosting Photocatalytic Hydrogen Generation. ACS Omega, 2021, 6, 13544-13553.	1.6	14
83	Potassium ferrate(VI) and decomposed K2FeO4 assisted methanol electro-oxidation in alkaline media. Electrochimica Acta, 2009, 54, 3548-3552.	2.6	13
84	Solubilities of Diglycolic Acid Esters at Temperatures Ranging from (343 to 363) K in Supercritical Carbon Dioxide. Journal of Chemical & Engineering Data, 2010, 55, 694-697.	1.0	13
85	Synthesis of halide anionâ€doped bismuth terephthalate hybrids for organic pollutant removal. Applied Organometallic Chemistry, 2016, 30, 304-310.	1.7	13
86	Composition-dependent dual halide anion-doped bismuth terephthalate hybrids for enhanced pollutants removal. Microporous and Mesoporous Materials, 2017, 244, 284-290.	2.2	13
87	Engineering amorphous red phosphorus onto ZnIn2S4 hollow microspheres with enhanced photocatalytic activity. Materials Letters, 2018, 232, 78-81.	1.3	13
88	β-Cyclodextrin/Quaternary Ammonium Salt as an Efficient Catalyst System for Chemical Fixation of CO <sub>2</sub> . Journal of Nanoscience and Nanotechnology, 2019, 19, 3263-3268.	0.9	13
89	AgBr Nanoparticles Anchored on CdS Nanorods as Photocatalysts for H <sub>2</sub> Evolution. ACS Applied Nano Materials, 2021, 4, 9274-9282.	2.4	13
90	A Simple Alcohothermal Synthetic Route to High Surface Area Zirconia Aerogel. Chemistry Letters, 2001, 30, 398-399.	0.7	12

#	Article	IF	CITATIONS
91	Efficient Solvent-Free Synthesis of Cyclic Carbonates from the Cycloaddition of Carbon Dioxide and Epoxides Catalyzed by New Imidazolinium Functionalized Metal Complexes Under 0.1ÂMPa. Catalysis Letters, 2020, 150, 2537-2548.	1.4	12
92	Facile one-step synthesis of quaternary AgInZnS quantum dots and their applications for causing bioeffects and detecting Cu2+. RSC Advances, 2020, 10, 9172-9181.	1.7	11
93	Er3+ doped bismuth oxychloride hierarchical microspheres with enhanced photocatalytic properties. Materials Letters, 2015, 158, 229-232.	1.3	10
94	Efficient Toluene Adsorption on Metal Salt-Activated Porous Carbons Derived from Low-Cost Biomass: A Discussion of Mechanism. ACS Omega, 2020, 5, 13196-13206.	1.6	10
95	Excellent photoreduction performance of Cr( <scp>vi</scp> ) over (WO <sub>4</sub> ) <sup>2â^²</sup> -doped metal organic framework materials. New Journal of Chemistry, 2020, 44, 20704-20714.	1.4	10
96	Self-assembled single-crystalline ZnO nanostructures. CrystEngComm, 2013, 15, 3780.	1.3	9
97	Self-Assembly of TiO <sub>2</sub> /CdS Mesoporous Microspheres with Enhanced Photocatalytic Activity via Hydrothermal Method. International Journal of Photoenergy, 2014, 2014, 1-10.	1.4	9
98	Synthesis and luminescence properties of hexagonal CaTiO3:Eu3+ nanosheets. Journal of Luminescence, 2014, 145, 144-147.	1.5	8
99	Bismuth terephthalate induced Bi(0) for enhanced RhB photodegradation and 4-nitrophenol reduction. Journal of Physics and Chemistry of Solids, 2017, 111, 431-438.	1.9	7
100	Emerging charge transfer in self-coupled polymorphs for promoting charge-carrier-involved photocatalysis. Chemical Engineering Journal, 2020, 396, 125213.	6.6	6
101	CdS Hollow Spheres Supported on Graphene Oxide Sheets with Enhanced Photocatalytic Activity. Science of Advanced Materials, 2013, 5, 1649-1657.	0.1	6
102	A distinct hollow spindle-like CdIn2S4 photocatalyst for high-efficiency tetracycline removal. Materials Today Chemistry, 2022, 24, 100800.	1.7	6
103	Multiple halide anion doped layered bismuth terephthalate with excellent photocatalysis for pollutant removal. RSC Advances, 2018, 8, 38370-38375.	1.7	5
104	Synthesis of Zn <i><sub>x</sub></i> Cd <sub>1–<i>x</i></sub> <i>S</i> Solid Solution Porous Spheres as Efficient Visible-Light Driven Photocatalysts. Science of Advanced Materials, 2013, 5, 1157-1167.	0.1	5
105	Urea-assisted synthesis of AlPO4:Ce,Tb nanorods as a redox luminescence switch. Journal of Nanoparticle Research, 2013, 15, 1.	0.8	4
106	Synthesis of quantum-sized BiOCl supported on SBA-16 with high dispersity and enhanced photocatalytic activity. Materials Letters, 2017, 205, 236-239.	1.3	4
107	Study on the resonance Raman scattering properties of β-carotene incorporated into SBA-15. Spectrochimica Acta - Part A: Molecular and Biomolecular Spectroscopy, 2010, 77, 518-521.	2.0	3
108	Hierarchical Ni–Co–O–C–P hollow tetragonal microtubes grown on Ni foam for efficient overall water splitting in alkaline media. RSC Advances, 2019, 9, 26051-26060.	1.7	3

Јинсненд Ни

#	Article	IF	CITATIONS
109	Pb2+ Responsive Cu-In-Zn-S Quantum Dots With Low Cytotoxicity. Frontiers in Chemistry, 2022, 10, 821392.	1.8	3
110	β-Carotene doped silicananoparticles as a novel resonance Raman scattering tag for in vivo cellular imaging. Journal of Materials Chemistry, 2012, 22, 631-635.	6.7	2
111	Synthesis and Photocatalytic Activity of Ultrafine SrNb6O16 Nanoparticles Supported on Graphene Oxide Nanosheets. Science of Advanced Materials, 2015, 7, 1331-1340.	0.1	2
112	INFLUENCE OF K <sup>+</sup> AND NA <sup>+</sup> IONS ON DIRECT ELECTROSYNTHESIS OF SOLID K <sub>2</sub> FEO <sub>4</sub> AND COMPARISON OF THE PHYSICOCHEMICAL PROPERTIES OF K <sub>2</sub> FEO <sub>4</sub> SAMPLES. Chemical Engineering Communications, 2012, 199, 178-188.	1.5	0